Sound & Vibration 2025, 59(2), 2600.
https://doi.org/10.59400/sv2600

Article

New scaling of critical damping and reduced frequency for mechanically excited systems

Md. Mahbub Alam

Mechanical and Automation Engineering Department, Harbin Institute of Technology (Shenzhen), Shenzhen 518055, China;
alamm28@yahoo.com, alam@hit.edu.cn

CITATION

Alam MM. New scaling of critical damping and reduced frequency for mechanically excited systems. Sound & Vibration. 2025; 59(2): 2600. https://doi.org/10.59400/sv2600

ARTICLE INFO

Received: 16 January 2025
Accepted: 12 March 2025
Available online: 18 March 2025

Abstract: This paper introduces a universal framework for understanding the vibration responses of systems subjected to harmonic excitation. By examining a simplified cylinder-spring-damper model, the study refurbishes traditional scaling methods for the excitation frequency ratio and critical damping ratio. The findings indicate that in damped systems, the maximum amplitude of vibration does not align with the natural frequency. This observation leads to the introduction of a new scaling method for reduced frequency. This new approach aligns resonance peaks at the new reduced velocity of 1.0 across different damping ratios, providing a consistent characterization of vibration behavior. A new critical damping ratio of 0.707 is identified for an excited system as opposed to the traditional damping ratio of 1.0 for an unexcited system. Key properties such as maximum amplitude, phase lag, bandwidth, and quality factor are analyzed, demonstrating that the proposed reduced frequency and critical damping ratio effectively capture the dynamics of both damped and undamped excited systems. The findings offer significant insights for practical applications in engineering and various scientific fields.

Keywords: damped vibration; excited system; frequency ratio; damping ratio; maximum amplitude

1. Introduction

All structures in nature and engineering possess mass, elasticity, and damping to some extent. They may, therefore, undergo vibration when subjected to harmonically excited forces (**Figure 1**). A harmonically excited system is susceptible to vibrating at the same frequency as the excitation. Harmonic excitation may be in the form of force or displacement of some points in the system. These excitation forces can arise from unbalanced rotating machines, reciprocating machines, the movement of a machine itself, earthquakes, bumps in the road, wind loading or Karman vortex shedding from a bluff body in a flow (**Figure 1**). The structural vibrations caused by these excitations essentially have the same fundamental physics governed by stiffness, damping, and excitation force [1]. While pure harmonic excitation is rare compared to periodic or other types of excitations, understanding how a system responds to harmonic excitation is essential for assimilating its response to various types of excitations. The vibration of a system is primarily influenced by the natural frequency of the system and the excitation frequency of the forces. The former remains approximately invariant, with minimal impact from damping [2]. In contrast, the excitation frequency of the excitation forces typically varies from low to high [3,4]. For example, when a car engine is started, the excitation frequency (engine rotation) increases from zero to about 16 Hz (1000 rpm), surpassing the natural frequency (1–2 Hz) of a car [5]. Most

washing machines have a drying speed of 800–1400 rpm (13–23 Hz), significantly higher than their natural frequencies. The frequency of vortex shedding from a bluff body increases almost linearly with increasing flow velocity [6,7]. Vortex-induced vibration often involves a "lock-in" phenomenon, where the vortex-shedding frequency synchronizes with the vibration frequency, known as resonance. In the lock-in regime, the vibration frequency may not necessarily match the natural frequency. For a low mass-damping ratio, the vibration frequency may be smaller or larger than the natural frequency when the excitation frequency is smaller and larger, respectively [3,4].

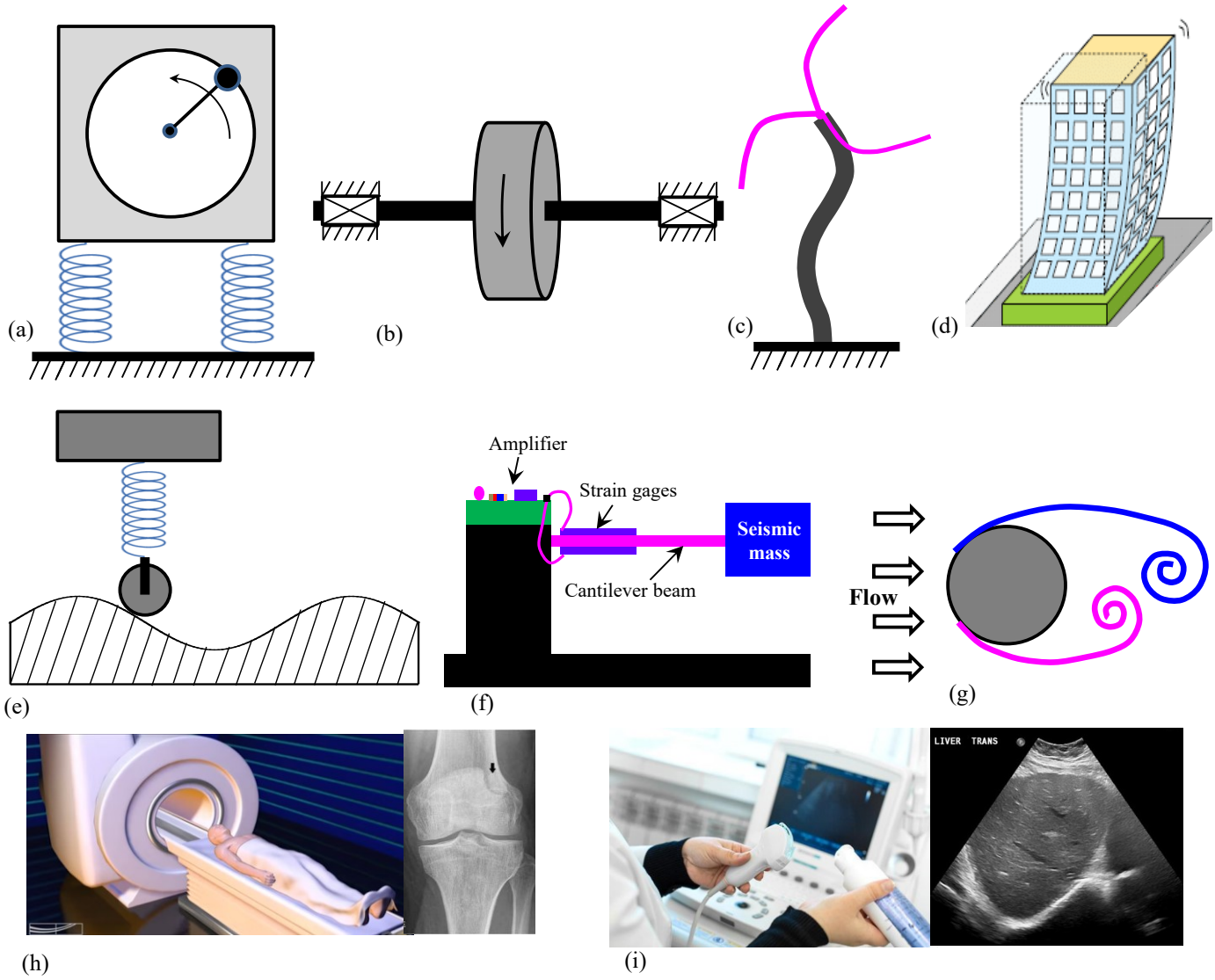

Figure 1. Structures undergo vibration when subjected to harmonically excited forces: **(a)** Unbalanced machines; **(b)** rotor or whirling shaft; **(c)** wind turbine tower and blades; **(d)** building subjected to earthquake; **(e)** automobile on road; **(f)** vibration sensor (piezoresistive accelerometer); **(g)** bluff-body subjected to flow; **(h)** magnetic resonance imaging (MRI) scanner; and **(i)** ultrasound imaging.

High-rise buildings and wind turbine towers or blades are no exception to the potential for large amplitude vibrations when the wind excitation or seismic (earthquake) frequency coincides with their natural frequencies. For example, when crossing a bridge, a marching army is often instructed to 'breakstep' so that each

soldier is out of step with the others to generate a much higher excitation frequency than the natural frequency of the bridge deck. This results in lower vibration amplitudes compared to all soldiers marching together in step. Understanding mechanical vibrations, fluid dynamics, fluid-structure interaction, and equipment involved is crucial in addressing these vibration problems. Failure to comprehend the vibration mechanism has led to many catastrophic events and futile vibration control.

Given the prevalence of excited oscillations in our daily life, from structural oscillations of suspension bridges or wind turbine blades/towers to the neural oscillations for perception (in brains), there is a critical need to study harmonic oscillations for pupils, teachers, and researchers in the fields of biology, chemistry, mathematics, physics, and engineering. As such, forced oscillations have been extensively studied and are generally well understood [8,9]. Yet, there may still be room to expand the fundamental knowledge on the topic.

A bluff body subjected to fluid flow undergoes fluctuating lift force because of alternate Karman vortex shedding from the bluff body (**Figure 1g**). The frequency of the fluctuating lift force matches the frequency of vortex shedding. The fluctuating lift force acts as the excitation force and the vortex shedding frequency as the excitation frequency. All these oscillations, driven by forces, can be classified as force oscillations.

Previous research has investigated the optimization of damping in mechanical systems and the effects of parametric excitation on system stability. Tomljanovic [10] developed an optimization approach for damper placement and viscosity selection in structures, aiming to maximize displacement decay. Their method accommodated both internal damping and multiple dampers with varying viscosities, using average displacement amplitude as the optimization criterion. In a different study, Arkhipova and Luongo [11] investigated how damping influences the parametric excitation-based stabilization of statically unstable linear Hamiltonian systems. Their analysis covered various resonance scenarios, including 1:1, 1:2, 2:1, and combination resonances (sum and difference). They discovered that while small amounts of damping could enhance control system performance, this benefit was limited to non-resonant conditions. Earlier works by Yabuno and Tsumoto [12] and Arkhipova et al. [13] revealed a trade-off in using parametric excitation for stabilization. While this approach can effectively stabilize an unstable mode, it simultaneously poses a risk to initially stable modes, potentially causing their destabilization through classical mechanisms.

Various methods exist for the estimation of structural damping, each with its own approach and applications. The classical Rayleigh model, employed by Scalzo et al. [14], offers one approach to characterizing damping behavior in test specimens. The half-power bandwidth method, utilized by Medel et al. [15] and Samimi et al. [16], involves applying harmonic forced vibrations to the structure and analyzing the response amplitude in the frequency domain. This technique provides a frequency-based assessment of damping characteristics. Perhaps the most straightforward approach is the logarithmic decrement method, as demonstrated in studies by Palmieri et al. [17] and He et al. [18]. This method operates under free vibration conditions, where the structure is initially displaced or given a velocity, and no external forces are applied during the measurement. The damping ratio is then determined by measuring the decay

rate of the structure's free response. The simplicity of this method makes it particularly attractive for practical applications.

Damped vibrations have diverse applications in medicine, including diagnostic imaging (ultrasound, MRI), medical devices, tissue engineering, and biomechanics (**Figure 1h,i**). Harnessing damping properties advances medical technology, diagnosis, and therapies [19,20]. For example, elastography uses damped vibrations to assess tissue stiffness, aiding in the diagnosis of conditions like liver cirrhosis and breast tumors. Biomechanics research analyzes damping in joints, bones, and soft tissues to improve rehabilitation, understand injuries, and optimize orthopedic implant design.

2. Problem definition and objective

The forced oscillation of a structure can be represented by a simplified system comprising a cylinder of mass m, a spring of stiffness k, and a damper of damping c (**Figure 2a**). Before applying the excitation force, it is assumed that the mass is in its static equilibrium where the upward spring force balances the downward gravity force. The displacement is measured from this static equilibrium. The cylinder is then excited by an external force $F = F_o\sin(\omega t + \phi)$, where F_o is the force amplitude, ω is the circular frequency (rad/s), t is the time and ϕ is the phase lag between the excitation force and the cylinder displacement (**Figure 2a**). Assume that the excitation force $F = F_o\sin(\omega t + \phi)$ results in the steady oscillation.

$$y = y_o\sin\omega t \tag{1}$$

where y_o is the amplitude of the cylinder displacement y. At time t measured from the static equilibrium position ($y = 0$), the free-body diagram of the cylinder is presented in **Figure 2b**, which leads to the following equation of motion.

$$m\ddot{y} + c\dot{y} + ky = F_o\sin(\omega t + \phi) \tag{2}$$

This equation is well-studied in textbooks on structural dynamics.

From Equations (1) and (2), we can get

$$\frac{y_o}{F_o/k} = A = \frac{1}{\sqrt{(1-r^2)^2 + (2\zeta r)^2}} \tag{3}$$

and

$$\phi = \tan^{-1}\frac{2\zeta r}{1-r^2} \tag{4}$$

where ζ (= $c/2m\omega_n$) is the damping ratio, r (= ω/ω_n) is the reduced frequency, also known as a frequency ratio, and ω_n (= $\sqrt{k/m}$) is the natural frequency. Equations (3) and (4) are well-known in textbooks. The $r = \omega/\omega_n$ is the standard normalization of the excitation frequency. The maximum amplitude, however, does not necessarily occur at $r = 1.0$ but at $r < 1.0$ when $\zeta > 0$ (Equation (3)). It does not correspond to the definition of resonance, suggesting that something is missing behind the normalization of the reduced frequency. The $\frac{y_o}{F_o/k} = A$ is the dimensionless oscillation amplitude on the scale of the spring deflection F_o/k caused by the force F_o applied statically. In other words, the A is a function of r and ζ. Several questions pop up: why does the

maximum A not correspond to resonance (r = 1.0)? Are the reduced frequency and damping ratio incongruously scaled or normalized? What is missing behind the scales? Although a structure with ζ < 1.0 is said to be underdamped, does it remain underdamped under excitation force? Does a peak in the A−r graph appear for all values of ζ < 1.0? If not, why not?

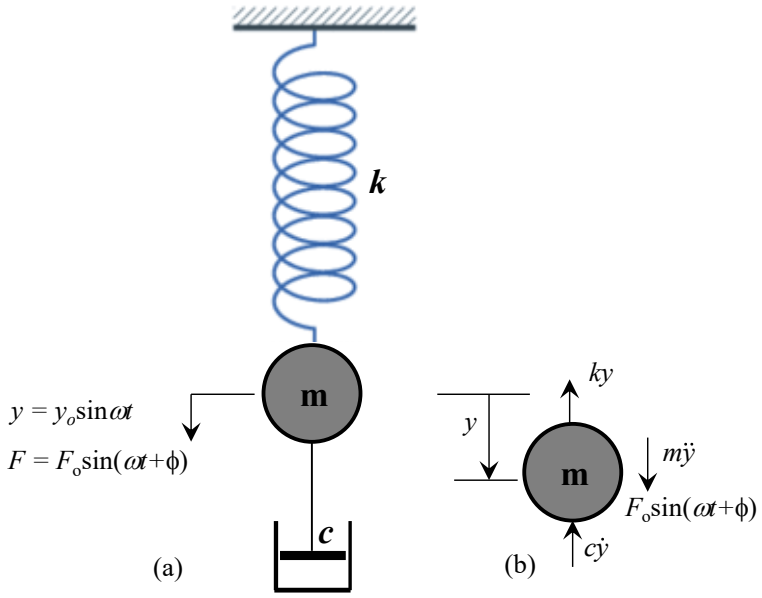

Figure 2. The forced oscillation of a structure: **(a)** Viscously damped cylinder system with harmonic excitation; and **(b)** free-body diagram of the cylinder.

We aim to provide a deeper understanding of the fundamentals of vibration responses of a forced damped system. Here, we introduce universal definitions of frequency ratio and critical damping ratio. It will be beneficial for teaching and learning the mechanics of a damped system undergoing excitation force. There is no doubt that this content is imperative and indispensable for pupils, teachers, researchers, engineers, and militaries.

3. Relationship between amplitude and reduced frequency

Figure 3a,d displays the relationship of A with r and ζ, as described by Equation (3). The frequency at which the amplitude peaks is called the resonant frequency. Resonance occurs at a critical reduced frequency $r_c = r = 1.0$ when $\zeta = 0$, resulting in A reaching infinity. As ζ increases, the peak in A becomes small and shifts to the left, i.e., $r_c < 1.0$ for $\zeta > 0$. In other words, the resonant frequency differs from the natural frequency when $\zeta \neq 0$. For example, the maximum (resonance) values of A are 5.02 (not visible in the figure), 3.37, 2.55, 1.75, 1.36, 1.15, 1.04, and 1.01 for ζ = 0.1, 0.15, 0.2, 0.3, 0.4, 0.5, 0.6, and 0.7, respectively, occurring at r_c = 0.989, 0.977, 0.959, 0.905, 0.824, 0.707, 0.529, and 0.141. The higher the ζ, the smaller the r_c. This observation contradicts the definition of resonance, which requires r_c = 1.0. This implies that r is not appropriately scaled in this case. For $\zeta \geq 0.8$, no peak emerges as A is less than 1.0 for $r > 0$. When $\zeta \leq 0.7$, A first increases from A = 1.0 at r = 0, peaks, then rapidly

declines to $A = 0.11$–0.19 at $r = 2.5$ and $A = 0.05$–0.06 at $r = 4.0$ depending on ζ. As r becomes very large, A tends to die down to zero for all values of ζ (**Figure 3c**). The impact of ζ on A is minimal when r is sufficiently large ($r > 4.0$) where the vibration amplitude is only 5% of the static deflection by the force amplitude. In other words, no damper is required if the system has $r > 4.0$.

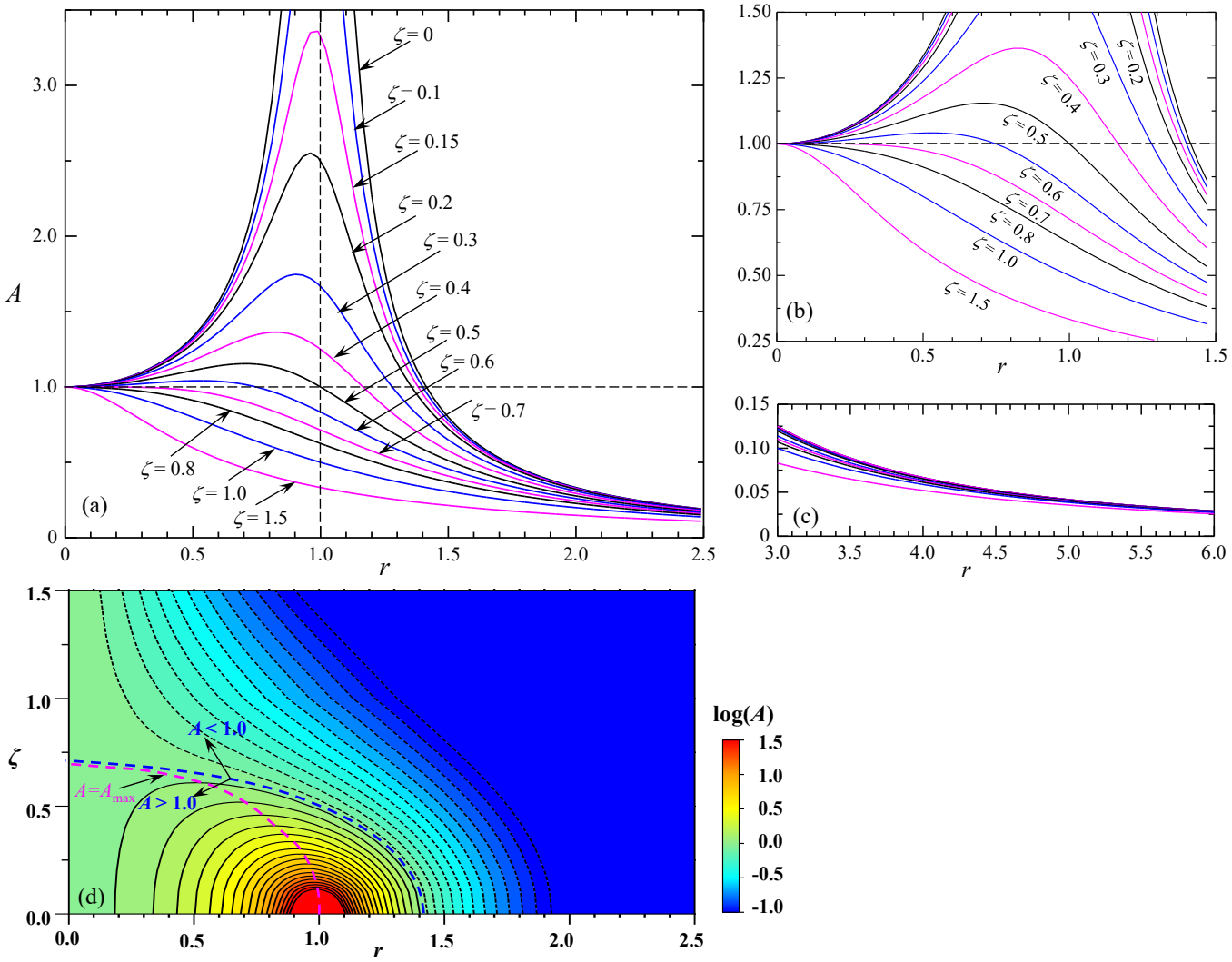

Figure 3. The relationship of A with r and ζ: **(a)** Steady state vibration amplitude A of an elastically mounted cylinder undergoing forced vibration; **(b)** zoomed-in view of **(a)**; **(c)** vibration amplitude A for large r values; and **(d)** contour plot of amplitude A on r–ζ plane.

Note: **(a)** As a function of excitation frequency ratio r and damping ratio ζ; **(b)** There are peaks in A for $\zeta \leq 0.7$ where the value of r corresponding to the peak A decreases with increasing ζ; **(c)** showing negligible influence of ζ on A; **(d)** the purple-dashed and blue-dashed lines mark the peak A (A_{max}) and $A = 1.0$, respectively, for each ζ value.

Typically, in engineering applications, a small or zero amplitude is desired. To achieve this, one should choose a large ζ value at small $r < 2.5$ and/or a large $r > 4.0$ where damping does not matter. The latter scenario requires that the excitation frequency significantly exceed the natural frequency. Although A at a high r is not highly affected by ζ, A crosses the $A = 1$ line at different r values depending on ζ; the higher the ζ, the smaller the r. Given that the resonance peak and crossing point

heavily both rely on ζ, an appropriate scaling of the excitation frequency is necessary to appropriately characterize the resonance and align amplitude peaks on a vertical line for various ζ values. Here, we fish out a way to appropriately scale the excitation frequency.

Let us understand the relationship between ζ and r_c first. For a given ζ, the A is maximum when the denominator $D = (1 - r^2)^2 + (2\zeta r)^2$ in Equation (3) is minimum.

To find the condition of r for a minimum D, we can set

$$\begin{aligned} &\frac{dD}{dr} = 0 \\ \Rightarrow\ &2(1 - r^2)(\text{-}2\text{r}) + 8\zeta^2 r = 0 \\ \Rightarrow\ &4r(r^2\text{-}1 + 2\zeta^2) = 0 \end{aligned} \tag{5}$$

$$\text{i.e., } r = 0$$

and/or

$$\begin{aligned} &r^2\text{-}1 + 2\zeta^2 = 0 \\ \Rightarrow\ &r^2\text{=}1\text{-}2\zeta^2 \\ \Rightarrow\ &r = r_c = \sqrt{1 - 2\zeta^2} \end{aligned} \tag{6}$$

As shown in **Figure 3** and as Equation (5) indicates, the slope of A is zero at r = 0 regardless of ζ, although r = 0 does not necessarily represent the maximum. On the other hand, Equation (6) indicates that D may be minimum (expected) or maximum for $r = \sqrt{1 - 2\zeta^2}$. To confirm whether D is maximum or minimum at r = 0 and $r = \sqrt{1 - 2\zeta^2}$, we can get the second derivative of D, i.e.,

$$\frac{d^2D}{dr^2} = 12r^2 - 4 + 8\zeta^2 \tag{7}$$

For r = 0, we can find that

$$\frac{d^2D}{dr^2} = -4(1 - 2\zeta^2) \tag{8}$$

It gives that $\frac{d^2D}{dr^2} = -ve$ for $0 < \zeta < 1/\sqrt{2}$ and $\frac{d^2D}{dr^2} = +ve$ for $\zeta > 1/\sqrt{2}$.

This suggests that there are two sets of curves originating at r = 0: one with positive curvature of D (i.e., negative curvature of A) and the other with negative curvature of D (i.e., positive curvature of A). The latter, with a positive curvature of A at r = 0, displays a peak at $r = r_c$ but the former does not (**Figure 3a**). Let us fish out this mathematically.

For $r = \sqrt{1 - 2\zeta^2}$, we can find that

$$\frac{d^2D}{dr^2} = 8(1 - 2\zeta^2) \tag{9}$$

Equation (9) gives $\frac{d^2D}{dr^2} = +ve$ (i.e., resonance or peak in A) only when

$$1 - 2\zeta^2 > 0$$

$$\Rightarrow \zeta < 1/\sqrt{2}; \text{ i.e., } \zeta < 0.707 \tag{10}$$

Again, there are two sets of curves: ones with $\zeta < 1/\sqrt{2}$ display a peak at $r = r_c = \sqrt{1-2\zeta^2}$ and the others with $\zeta > 1/\sqrt{2}$ have no peaks, where A monotonically declines with increasing r. For $\zeta = 1/\sqrt{2}$, we get $\frac{d^2D}{dr^2} = 0$, which indicates a stationary inflection point at $r = 0$.

That is, $\zeta = 1/\sqrt{2} = \zeta_c$ is a critical damping ratio that separates the resonance with a peak in amplitudes ($A > 1.0$) from the no resonance ($A < 1.0$). The $\zeta > \zeta_c$ $(= 1/\sqrt{2})$ essentially signifies that the system is overdamped. This should not be confused with the underdamping $\zeta < 1.0$, critical damping $\zeta = 1.0$, and over-damping $\zeta > 1.0$; all of which refer to an unexcited system. Here, we propose a universal critical damping ratio of $\zeta_c = 1/\sqrt{2}$ for excited systems including damped and undamped systems.

It is worth understanding the origin of this universal critical damping ratio $\zeta_c = 1/\sqrt{2}$. We know that a system with damping has a smaller damped natural frequency, i.e.,

$$\omega_d = \omega_n\sqrt{1-\zeta^2} \tag{11}$$

Since the damped natural frequency ω_d is smaller than the ω_n, the critical damping of the damped system is reduced to

$$c_{cd} = 2m\omega_d = 2m\omega_n\sqrt{1-\zeta^2} = c_c\sqrt{1-\zeta^2} \tag{12}$$

where $c_c = 2m\omega_n$ is the critical damping of the unexcited system, where the vibration is applicable for a damping ratio less than one, i.e., an underdamped case. As such, the critical damping ratio $\zeta = 1.0$, which is based on $c_c = 2m\omega_n$, is not valid anymore for an excited system with damping, because ζ becomes larger than one when the critical damping of the damped system is taken into account. Considering the critical damping of the damped system, we can write the damping ratio of the damped system as

$$\zeta_d = \frac{c}{c_{cd}} = \frac{c}{2m\omega_n\sqrt{1-\zeta^2}} = \frac{2m\omega_n\zeta}{2m\omega_n\sqrt{1-\zeta^2}} = \frac{\zeta}{\sqrt{1-\zeta^2}} \tag{13}$$

To have resonance, $\zeta_d < 1$ (underdamping), viz.,

$$\begin{aligned} &\frac{\zeta}{\sqrt{1-\zeta^2}} < 1 \\ &\Rightarrow \zeta^2 < 1-\zeta^2 \\ &\Rightarrow 2\zeta^2 < 1 \\ &\text{i.e., } \zeta < 1/\sqrt{2} \end{aligned} \tag{14}$$

In other words, there is no resonance (no peak) for $\zeta > 1/\sqrt{2}$ but is for $\zeta < 1/\sqrt{2}$ (**Figure 3**). The excitation fails to excite vibration when $\zeta > 1/\sqrt{2}$. It can, therefore, be said that $\zeta_c = 1/\sqrt{2}$ is a new critical damping ratio distinguishing the occurrence of resonance from the no resonance.

Figure 4 shows the dependence of r_c on ζ (Equation (6)). The r_c declines rapidly from 1.0 to 0 for $\zeta < 1/\sqrt{2} = 0.707$ while it remains zero for $\zeta > 1/\sqrt{2} = 0.707$. The new critical damping ratio $\zeta_c = 1/\sqrt{2} = 0.707$.

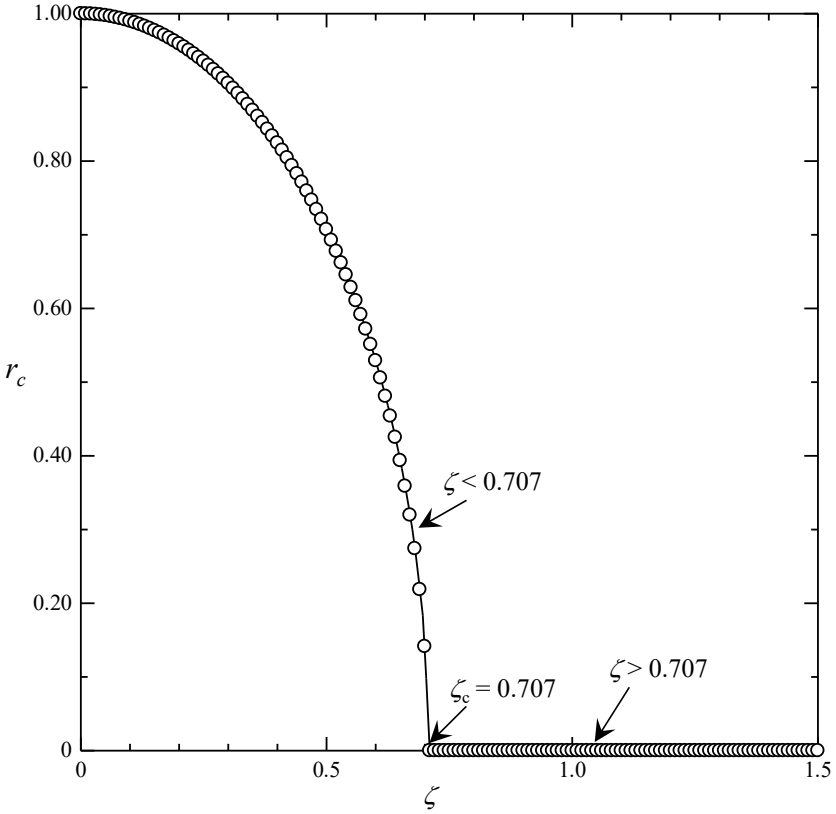

Figure 4. Dependence of the new critical reduced frequency r_c on damping ratio ζ.

4. Scaling of reduced frequency

Figure 3 demonstrates that the resonance does not coincide with $r = 1.0$ for all ζ values except $\zeta = 0$. In addition, it has been shown above that adding damping to the system modifies the natural frequency of the damped system. Therefore, the modified natural frequency of the damped system should be considered to scale the excitation frequency. Given that the damping ratio of the damped system is $\zeta_d = \zeta / \sqrt{1-\zeta^2}$, one can find the new damped natural frequency.

$$\begin{aligned} \omega_{dn} &= \omega_d \sqrt{1-\zeta_d^2} \\ &= \omega_n \sqrt{1-\zeta^2}\sqrt{1-\zeta^2/(1-\zeta^2)} \\ &= \omega_n \sqrt{1-2\zeta^2} \end{aligned} \tag{15}$$

$$\text{i.e., } \omega_{dn} = \omega_n \sqrt{1-2\zeta^2}$$

We can now find the new reduced frequency as

$$r_d = \frac{\omega}{\omega_{dn}} = \frac{\omega}{\omega_n \sqrt{1-2\zeta^2}} = \frac{r}{\sqrt{1-2\zeta^2}} = \frac{r}{r_c} \tag{16}$$

The r_d is now appropriately scaled reduced frequency. The relationship of r_d with r for different ζ values (Equation 16) is graphed in **Figure 5**. The r_d is a linear function of r with a steeper slope for a higher ζ. The impact of ζ on r_d is small for $\zeta < 0.2$, with r_d increasing 4.2% only between $\zeta = 0$ and 0.2. On the other hand, the impact is more significant for larger ζ (> 0.2) values.

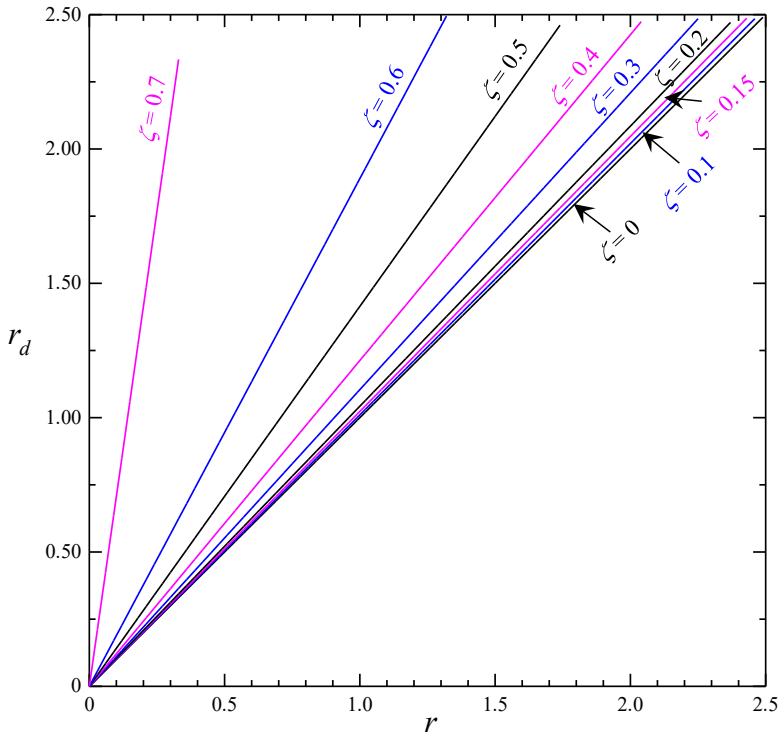

Figure 5. Relationship of the new reduced frequency r_d with the classical reduced velocity r and ζ.

To see the potential of r_d to act as the appropriately scaled frequency, the amplitude curves in **Figure 3** are now plotted against r_d in **Figure 6a**. The peaks are now aligned at $r_d = 1.0$ for all values of ζ (< 0.707), and all intersections for $A < 1.0$ converge at $r_d = \sqrt{2} = 1.414$. This implies that the excitation frequency should be scaled as r_d, rather than as r. The newly proposed reduced frequency r_d brings in the occurrence of the resonances at $r_d = 1.0$ for all ζ values below the new critical damping $\zeta_c = 0.707$. The newly defined r_d is, therefore, said to be universal reduced frequency. **Figure 6b** displays a contour plot of log-transformed A data presented in **Figure 6a**. The location of peak A is indicated by a purple-dashed line, while $A = 1.0$ ($\log(A) = 0$) is represented by a blue-dashed line for each ζ value. At a given r_d value, A declines and grows with increasing ζ when $r_d < \sqrt{2}$ and $r_d > \sqrt{2}$, respectively. This suggests that a smaller ζ is more favorable for suspending a structure when $r_d > \sqrt{2}$. Notably, the highly curved A_{max} and $A = 1.0$ lines observed in the r–ζ plane in **Figure 3d** appear as straight vertical lines in the r_d–ζ plane in **Figure 6b**. This transformation highlights the potential, significance, and universality of the newly defined r_d for both excited and unexcited systems.

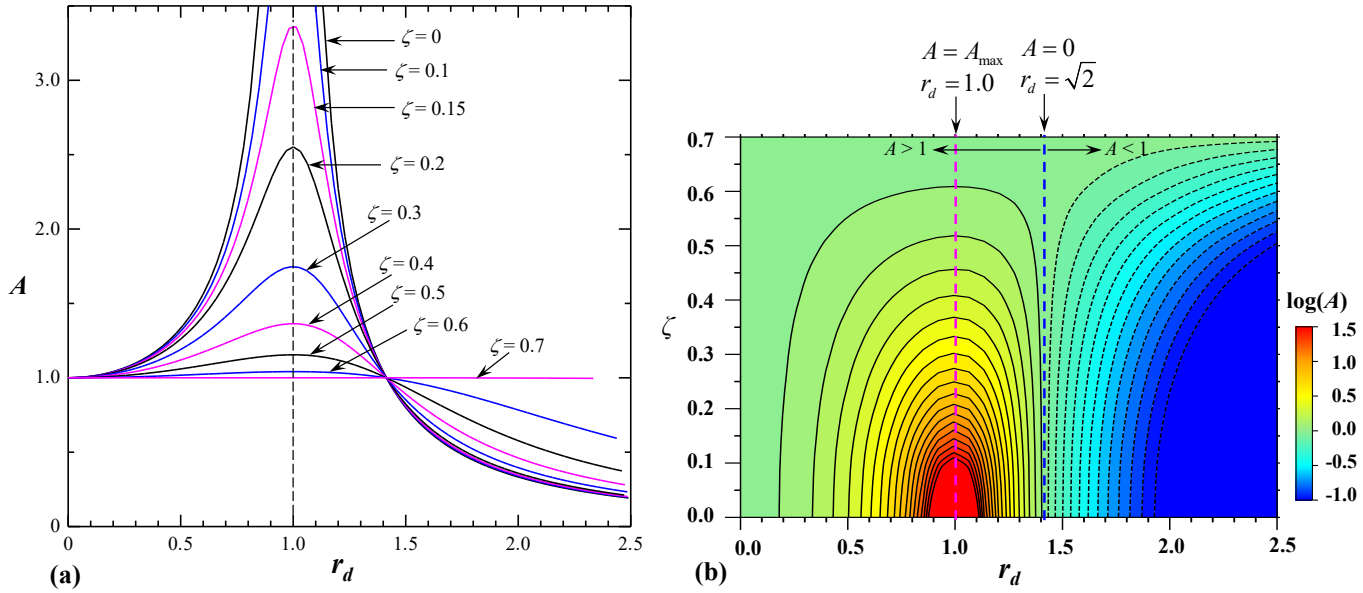

Figure 6. The relationship of A with r and ζ, with r_d acting as the appropriately scaled frequency: **(a)** Steady-state vibration amplitude A of an elastically mounted cylinder undergoing forced vibration as a function of the new reduced frequency r_d and damping ratio ζ; **(b)** Contour plot of amplitude A on the r_d–ζ plane.

Note: **(a)** The resonance peaks in A for $\zeta \leq 0.7$ are now on a vertical line $r_d = 1.0$, and all crossing points collapse into $r_d = 1.414$; **(b)** the purple-dashed and blue-dashed lines mark the peak A (A_{max}) and $A = 1.0$, respectively, for each ζ value.

Let us see how the vibration response equation looks when the r_d is introduced in Equation (3). From Equations (3) and (16), we can write

$$A = \frac{1}{\sqrt{\{1 - r_d^2 r_c^2\}^2 + (2\zeta r_d r_c)^2}} \tag{17}$$

Using Equation (16), it can further be expanded as

$$\begin{aligned} A &= \frac{1}{\sqrt{\{1 - r_d^2(1 - 2\zeta^2)\}^2 + 4\zeta^2 r_d^2(1 - 2\zeta^2)}} \\ &= \frac{1}{\sqrt{1 - r_d^2(1 - 2\zeta^2)\{2 - r_d^2(1 - 2\zeta^2) - 4\zeta^2\}}} \\ &= \frac{1}{\sqrt{1 - r_d^2(2 - r_d^2)(1 - 2\zeta^2)^2}} \end{aligned} \tag{18}$$

$$\text{i.e., } A = 1/\sqrt{1 - r_d^2(2 - r_d^2)(1 - 2\zeta^2)^2}$$

Equation (18) reflects that, regardless of ζ, the A is maximum at $r_d = 1.0$ while $A < 1.0$ for $r > \sqrt{2}$ (crossing point). Equation (18) and **Figure 6** further reflect that $A = 1.0$ for $r_d = 0$ and $r_d = \sqrt{2} = 1.414$.

Ibrahim [21] investigated the impact of nonlinear spring behavior on forced vibration amplitude through a comprehensive parametric study. His findings revealed

notable distinctions in the system's response compared to systems with purely linear springs. Specifically, the introduction of a nonlinear component resulted in a shift of the system's resonance frequency, deviating by approximately ten percent from the linear case. Furthermore, a qualitative change in the system's response curve was observed; the nonlinearity caused the curve to bend over at high amplitudes, effectively limiting and forcing down the system's response. This behavior was attributed to the nonlinear spring's influence, leading to resonance peaks occurring at higher frequencies compared to a linear system. A thorough validation of the new scaling method's applicability across diverse nonlinear scenarios is essential for future investigations.

5. Novelty and advantages of the new critical damping ratio and reduced velocity

Traditional methods like the Rayleigh damping model [14] and the half-power bandwidth method [15] rely on classical reduced frequency r (= ω/ω_n) and damping ratio ζ for resonance characterization. However, these methods fail to align resonance peaks accurately across different damping ratios. This paper introduces a new reduced frequency $r_d = \omega/(\omega_n\sqrt{1-2\zeta^2})$, which consistently aligns resonance peaks at r_d = 1.0 and the crossing points A = 1.0 (beyond resonance) at $r_d = \sqrt{2}$, regardless of ζ. This refinement offers a more accurate characterization of vibration behavior, particularly for damped systems.

Techniques like the logarithmic decrement method [17] and parametric excitation-based stabilization [11] are effective but limited to specific scenarios, such as free vibration or non-resonant conditions. The new scaling for reduced frequency and critical damping ratio is universally applicable, capturing the dynamics of both damped and undamped excited systems. This makes it suitable for a broader range of engineering applications, from mechanical systems to biomechanics and medical imaging [19], where damping properties play a critical role. While methods like damper optimization [10] and vibration fatigue analysis [17] are practical, they often require complex calculations or experimental setups. The framework simplifies the characterization of the resonance by collapsing peaks at a consistent reduced frequency (r_d = 1.0). This reduces computational complexity and enhances practical implementation in real-world systems, such as automotive suspensions, structural engineering, and medical devices.

For unexcited systems, stability is classified as underdamped (ζ < 1.0), critically damped (ζ = 1.0), or overdamped (ζ > 1.0). However, this classification does not account for the presence of external excitation forces. Our new critical damping ratio $\zeta_c = 1/\sqrt{2}$ serves as a threshold for resonance in excited systems. Firstly, for $\zeta < \zeta_c$, the system is underdamped and resonant, exhibiting a peak in the amplitude-frequency response at r_d = 1.0 for all values of $\zeta < \zeta_c$. Secondly, for $\zeta \geq \zeta_c$, the system is non-resonant, with no peak in the amplitude-frequency response. The amplitude-frequency curve monotonically declines, which is critical for applications like vibration isolation systems or shock absorbers, where minimizing amplitude at all frequencies is desired. This behavior is crucial for designing systems where resonance must be avoided, such

as aerospace structures, bridge engineering, vibration isolation systems, and shock absorbers.

The new critical damping ratio can be used to optimize damping in car suspensions. For instance, when $\zeta < \zeta_c$, the suspension system can absorb road vibrations without excessive oscillations, improving ride comfort. Conversely, when $\zeta \geq \zeta_c$, the system ensures that oscillations are minimized, enhancing stability at high speeds. In the cases of wind turbine blades, suspension bridges, or ocean risers, ζ_c can help determine the damping required to prevent resonance caused by vortex-induced vibrations. By adjusting ζ to be slightly above ζ_c, the mentioned structures can operate efficiently without excessive resonant oscillations. In ultrasound imaging or elastography, $\zeta_c$can be applied to design transducers that achieve optimal damping, ensuring accurate imaging without distortion from resonant vibrations. In seismic design, $\zeta_c$can guide the selection of damping materials to ensure that buildings remain stable during earthquakes. For $\zeta < \zeta_c$, structures can absorb seismic energy, while $\zeta \geq \zeta_c$ can completely prevent resonance-induced damage. By further exploring the impact of the new reduced velocity and critical damping on system stability and frequency response and illustrating their application through practical case studies, the theory can be solidified as a fundamental tool for vibration analysis across diverse engineering disciplines. This would not only enhance the theoretical framework but also bridge the gap between theory and practical implementation.

6. Properties of response curves

Four predominant properties feature the vibration responses in **Figure 6**: maximum vibration amplitude $A_{\max}$, phase lag ϕ between force and displacement, sharpness or bandwidth $(\Delta r_d)_b = r_{d2} - r_{d1}$ of the responses, and quality factor Q. The $A_{\max}$ and ϕ are easily understood while the $(\Delta r)_b$ is the width of r corresponding to the amplitude of $A_{\max}/\sqrt{2}$ representing power or root-mean-square of displacement at the resonance. The quality factor, also known as the Q factor, is the ratio of the initial energy stored in the resonator to the energy lost in one radian of the oscillation cycle, indicating the degree of damping of an oscillator or resonator [22]. It is alternatively defined as the ratio of the resonance frequency to its bandwidth when subjected to an oscillating driving force. These two definitions are numerically similar at small damping but differ at high damping. A higher Q indicates a lower rate of energy loss, and the oscillations die out more slowly. In other words, resonators with high-quality factors have low damping [23]. All three are essentially a measure of the damping in a system.

Maximum amplitude: We have found that maximum vibration amplitude $A_{\max}$ occurs at $r_d = 1.0$. Plugging $r_d = 1.0$ in Equation (18), we can get

$$A_{\max} = \frac{1}{2\zeta\sqrt{1-\zeta^2}} \tag{19}$$

The dependence of $A_{\max}$on ζ is illustrated in **Figure 7**. The $A_{\max}$ is highly sensitive to $\zeta$for $\zeta < 0.4$ where $A_{\max}$ plunges from ∞ to 1.75 with ζincreasing from 0

to 0.3. On the other hand, when ζ is increased from 0.3 to 0.7, the $A_{\max}$ decreases much less, from 1.75 to 1.0 only. When ζ is small, the maximum amplitude can be reduced to

$$A_{\max} = \frac{1}{2\zeta} \tag{20}$$

Equation (20) indicates that $A_{\max}$ declines hyperbolically with increasing ζ (see the inset of **Figure 7**).

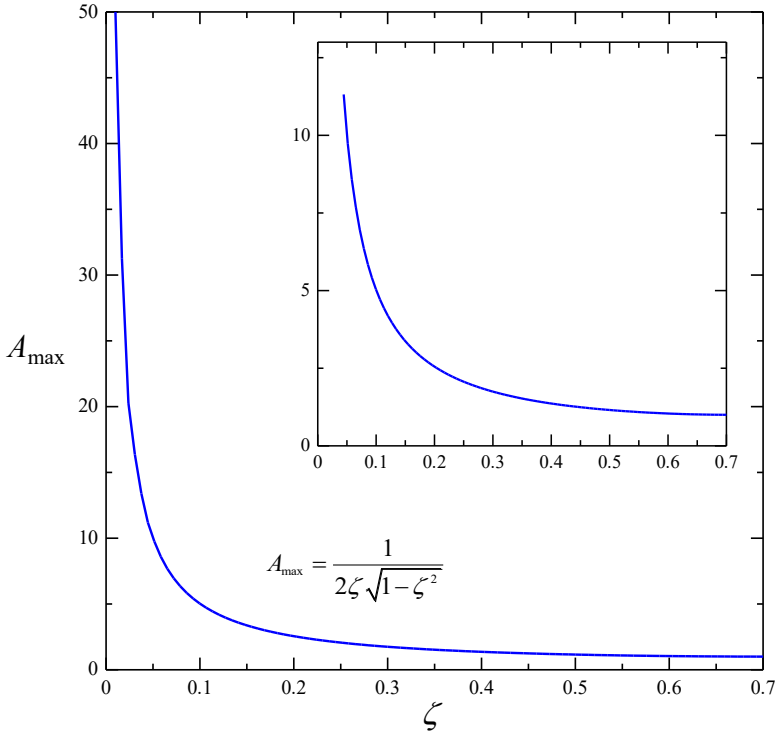

Figure 7. Dependence of maximum amplitude $A_{\max}$ on damping ratio ζ.

Note: The inset is a zoomed-in view; The amplitude declines rapidly for $\zeta < 0.3$ and mildly for $\zeta > 0.3$.

Phase lag at maximum amplitude: It is known that $\phi = 90°$ at the resonance (maximum A) when ζ is small. Is it true when ζ is large? It is thus worth finding the dependence of ϕ at the maximum amplitude ($r_d = 1.0$) on ζ, as shown in **Figure 8**. With increasing ζ from 0 to 0.6, the phase lag corresponding to the resonance (maximum amplitude) decreases from 90° to 41.4°. This implies that the phase lag is not necessarily 90°, but less than 90°, at the resonance for a high damping ratio. In classical flow-induced vibrations of a bluff body, it is a well-accepted argument that $\phi < 90°$ and $\phi > 90°$ in the initial/upper and lower branches of the vibration response curve, respectively, with $A_{\max}$ corresponding to $\phi \approx 90°$ [4,24]. **Figure 8**, nevertheless, reflects that the case of $\phi < 90°$ and $\phi > 90°$ in the initial/upper and lower branches, respectively, may be true when the damping ratio is as small as $\zeta < 0.05$. The lower branch or a part of the lower branch may have $\phi < 90°$ when the damping ratio is large.

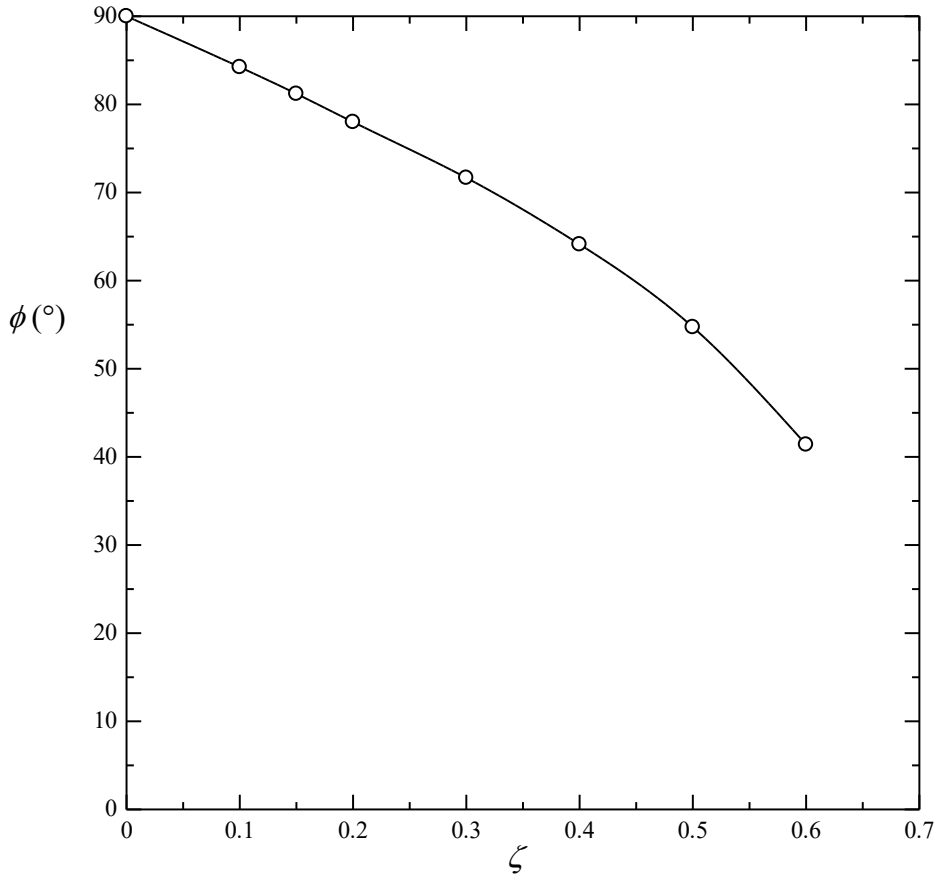

Figure 8. Dependence of phase lag ϕ at maximum amplitude $A_{\max}$ on the damping ratio ζ (< 0.7).

Bandwidth and quality factor: Putting the value of $A = A_{\max}/\sqrt{2} = \frac{1}{2\sqrt{2}\zeta\sqrt{1-\zeta^2}}$ in Equation (18), we can get

$$\frac{1}{2\sqrt{2}\zeta\sqrt{1-\zeta^2}} = \frac{1}{\sqrt{1-r_d^2(2\text{-}r_d^2)(1\text{-}2\zeta^2)^2}}$$
$$\Rightarrow 8\zeta^2(1-\zeta^2) = 1-(2r_d^2-r_d^4)(1\text{-}2\zeta^2)^2$$
$$\Rightarrow 8\zeta^2-8\zeta^4 = 1-2r_d^2(1\text{-}2\zeta^2)^2+r_d^4(1\text{-}2\zeta^2)^2$$
$$\Rightarrow r_d^4(1\text{-}2\zeta^2)^2-2r_d^2(1\text{-}2\zeta^2)^2+1\text{-}8\zeta^2+8\zeta^4 = 0$$
$$\Rightarrow r_d^4-2r_d^2+\frac{1\text{-}8\zeta^2+8\zeta^4}{(1\text{-}2\zeta^2)^2} = 0$$

It leads to two solutions r_{d1} and r_{d2} of r_d, i.e.,

$$r_{d1} = \left\{1-\frac{2\zeta\sqrt{1-\zeta^2}}{1\text{-}2\zeta^2}\right\}^{1/2} \tag{21a}$$

$$r_{d2} = \left\{1+\frac{2\zeta\sqrt{1-\zeta^2}}{1\text{-}2\zeta^2}\right\}^{1/2} \tag{21b}$$

From Equation (21),

$$r_{d2}^2 - r_{d1}^2 = \frac{4\zeta\sqrt{1-\zeta^2}}{1\text{-}2\zeta^2}$$

$$\Rightarrow (r_{d2} + r_{d1})(r_{d2} - r_{d1}) = \frac{4\zeta\sqrt{1-\zeta^2}}{1\text{-}2\zeta^2} \tag{22}$$

$$\Rightarrow \frac{(r_{d2} + r_{d1})}{2}(r_{d2} - r_{d1}) = \frac{2\zeta\sqrt{1-\zeta^2}}{1\text{-}2\zeta^2}$$

Considering each curve is symmetric about $r_d = r_{dc}$ =1.0, we can write (r_{d1}+ r_{d2})/2 = 1.0 which makes Equation (22) as

$$r_{d2} - r_{d1} = \frac{2\zeta\sqrt{1-\zeta^2}}{1\text{-}2\zeta^2} \tag{23}$$

which is the bandwidth of the response.

The quality factor is defined as

$$Q = \frac{r_{dc}}{r_{d2} - r_{d1}} = \frac{1\text{-}2\zeta^2}{2\zeta\sqrt{1-\zeta^2}} \tag{24}$$

Equations (19) and (24) echo that the larger the ζ, the smaller the Q and $A_{\max}$.

If ζ is small, the r_{d1}, r_{d2} and Q can be reduced to

$$r_{d1} = \{1 - 2\zeta\}^{1/2}, \tag{25a}$$

$$r_{d2} = \{1 + 2\zeta\}^{1/2}, \text{ and} \tag{25b}$$

$$Q = \frac{r_{dc}}{r_{d2} - r_{d1}} = \frac{1}{2\zeta} \tag{25c}$$

All these features for small ζ are reflected in **Figure 9**. Equations (20) and (25c) both are with an assumption of small ζ, yielding $Q = A_{\max} = 1/(2\zeta)$, i.e., Q essentially equals $A_{\max}$ at small ζ. It is, nevertheless, not the case when ζ is large. To assimilate the quantitative difference between Q and $A_{\max}$ for large values of ζ, $Q/A_{\max} = 1-2\zeta^2$ is presented in **Figure 10**, which reflects that $Q \approx A_{\max}$ for $\zeta < 0.05$ while Q is progressively smaller than $A_{\max}$ for $\zeta > 0.05$. That is, with increasing ζ, the Q decays more rapidly than the $A_{\max}$, the former being only 2% of the latter at $\zeta = 0.7$.

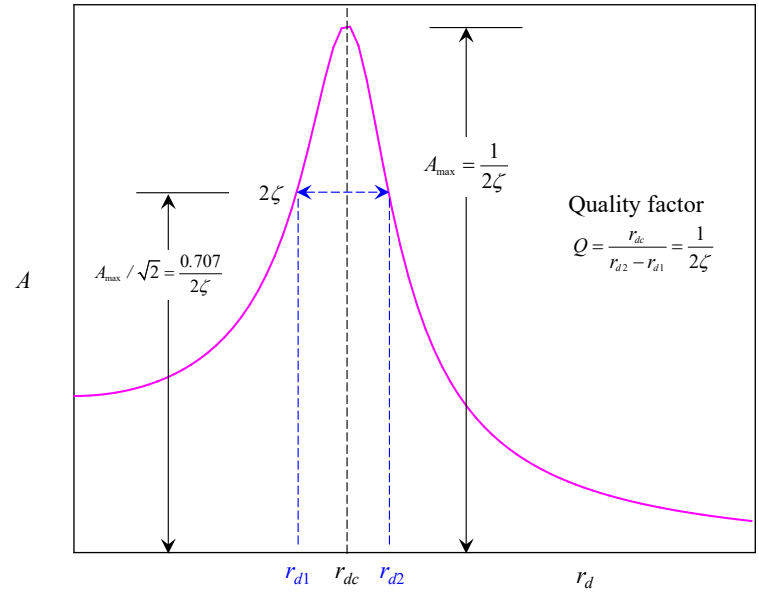

Figure 9. Shape function for a vibration mode and its features.

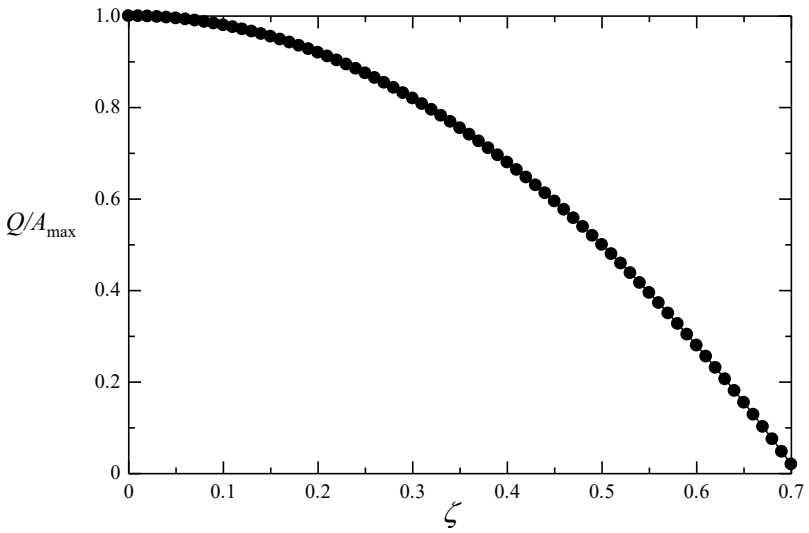

Figure 10. Ratio of Q and A_{max} for different ζ values. The $Q/A_{max} \approx 1.0$ for $\zeta < 0.05$ while it decreases parabolically for $\zeta > 0.05$.

7. Conclusions

The paper explores the fundamental principles of vibrations in systems subjected to harmonic excitation. The study models a forced oscillation using a cylinder-spring-damper system. Key questions include why maximum amplitude does not align with resonance and how damping and frequency are scaled. The goal is to provide a universal understanding of damped systems under excitation.

The amplitude A of vibration depends on the damping ratio (ζ) and the reduced frequency (r). The impact of ζ on A is insignificant for $r > 4.0$ but significant for $r < 2.0$. The so-called resonance occurs at $r = 1.0$ only for undamped systems ($\zeta = 0$). For damped systems, the resonance (peak amplitude) shifts to $r < 1.0$ for $\zeta < 1/\sqrt{2}$ and the resonance is absent for $\zeta > 1/\sqrt{2}$. This study imparts a new critical damping ratio of $\zeta = \zeta_c = 1/\sqrt{2}$ for an excited system becoming underdamped for $\zeta < 1/\sqrt{2}$ and

overdamped for $\zeta > 1/\sqrt{2}$, respectively, as opposed to ζ = 1.0, < 1.0 and > 1.0 for an unexcited system, respectively. The study suggests that the traditional scaling of frequency is inadequate to define the resonance. A new scaling method for reduced frequency, denoted as $r_d = \omega/(\omega_n\sqrt{1-2\zeta^2}) = r/\sqrt{1-2\zeta^2}$, is proposed. This method aligns the resonance peaks at $r_d = 1.0 = r_c$ for different damping ratios, offering a more accurate characterization of vibration responses.

Four key properties—maximum amplitude, phase lag, bandwidth and quality factor—are discussed. The maximum amplitude decreases with increasing ζ as $A_{\max} = 1/(2\zeta\sqrt{1-\zeta^2})$. The phase lag at the resonance is not necessarily 90°, rather decreasing from 90° to 41.4° with increasing ζ from 0 to 0.6. The bandwidth of the frequency range is inversely related to damping. The relationship between quality factor Q decreases more rapidly for higher ζ values.

The paper concludes that the new definitions for critical damping ratio and reduced frequency provide a more universal framework for understanding and predicting the behavior of excited damped systems. Validation studies should be conducted across a range of applications to ensure the robustness and generalizability of the findings.

Funding: The author wishes to acknowledge support from NSFC through grant 12472235.

Conflict of interest: The author declares no conflict of interest.

References

1. Tse FS, Morse IE, Hinkle RT. Mechanical Vibrations: Theory and Applications, 2nd ed. Allyn and Bacon, Inc.; 1978.
2. Alam MM. A note on flow-induced force measurement of oscillating cylinder by loadcell. Ocean Engineering. 2022; 245: 110538. doi: 10.1016/j.oceaneng.2022.110538
3. Bhatt R, Alam MM. Vibrations of a square cylinder submerged in a wake. Journal of Fluid Mechanics. 2018; 853: 301–332. doi: 10.1017/jfm.2018.573
4. Lin C, Alam MM. Intrinsic features of flow-induced stability of square cylinder. Journal of Fluid Mechanics. 2024; 988: A50. doi: 10.1017/jfm.2024.445
5. Sharma S, Chouksey M, Pare V, Jain P. Modal and frequency response characteristics of vehicle suspension system using full car model. In: Proceedings of the 2nd International Conference on Emerging trends in Manufacturing, Engines and Modelling (ICEMEM-2019); 23–24 December 2019; Mumbai, India.
6. Bai H, Alam MM. Dependence of square cylinder wake on Reynolds number. Physics of Fluids. 2018; 30(1). doi: 10.1063/1.4996945
7. Alam MM. Fluid force, moment and torque measurements of oscillating prism and cylinder using loadcell. Physics of Fluids. 2022; 34(12). doi: 10.1063/5.0124800
8. Glaister P, Glaister EM. HMS-harmonic motion by shadows. Teaching Mathematics and its Applications. 2009; 28(1): 10–15.
9. Kougias IE. Solving second-order ordinary differential equations without using complex numbers. Teaching Mathematics and its Applications. 2009; 28(2): 101–108. doi: 10.1093/teamat/hrp007
10. Tomljanovic Z. Damping optimization of the excited mechanical system using dimension reduction. Mathematics and Computers in Simulation. 2023; 207: 24–40. doi: 10.1016/j.matcom.2022.12.017
11. Arkhipova IM, Luongo A. On the effect of damping on the stabilization of mechanical systems via parametric excitation. Zeitschrift für angewandte Mathematik und Physik. 2016; 67: 69. doi: 10.1007/s00033-016-0659-6

12. Yabuno H, Tsumoto K. Experimental investigation of a buckled beam under high-frequency excitation. Archive of Applied Mechanics. 2007; 77(5): 339–351. doi: 10.1007/s00419-007-0112-6
13. Arkhipova IM, Luongo A, Seyranian AP. Vibrational stabilization of the upright statically unstable position of a double pendulum. Journal of Sound and Vibration. 2012; 331(2): 457–469. doi: 10.1016/j.jsv.2011.09.007
14. Scalzo F, Totis G, Vaglio E, Sortino M. Experimental study on the high-damping properties of metallic lattice structures obtained from SLM. Precision Engineering. 2021; 71: 63–77. doi: 10.1016/j.precisioneng.2021.02.010
15. Medel F, Abad J, Esteban V. Stiffness and damping behavior of 3D printed specimens. Polymer Testing. 2022; 109: 107529. doi: 10.1016/j.polymertesting.2022.107529
16. Samimi AH, Karamooz-Ravari MR, Dehghani R. Numerical and Experimental Investigation of Natural Frequency and Damping Coefficient of Flexible Cellular Lattice Structures. International Journal of Advanced Design and Manufacturing Technology. 2024; 17(1): 29–38.
17. Palmieri M, Zucca G, Morettini G, et al. Vibration fatigue of FDM 3D printed structures: The use of frequency domain approach. Materials. 2022; 15(3): 854. doi: 10.3390/ma15030854
18. He F, Ning H, Khan M. Effect of 3D Printing Process Parameters on Damping Characteristic of Cantilever Beams Fabricated Using Material Extrusion. Polymers. 2023; 15(2): 257. doi: 10.3390/polym15020257
19. Tabatabai H, Oliver DE, Rohrbaugh JW, Padadopoulos C. Novel Applications of Laser Doppler Vibration Measurements to Medical Imaging. Sensing and Imaging: An International Journal. 2013; 14(1–2): 13–28. doi: 10.1007/s11220-013-0077-1
20. Ghemari Z. Exploring Forced-damped Vibrations: Analysis, Modeling, and Medical Applications. Journal of Material Sciences & Applied Engineering. 2024; 3(1): 1–8.
21. Ebrahim M. Analyzing the numerical behavior of a vibration system with non-linearity using single degree of freedom approach. Journal of Mechanical Engineering and Automation. 2023; 12(2): 36–50. doi: 10.5923/j.jmea.20231202.02
22. Torvik PJ. On estimating system damping from frequency response bandwidths. Journal of Sound and Vibration. 2011; 330(25): 6088–6097. doi: 10.1016/j.jsv.2011.06.027
23. Thomson WT. Theory of Vibration with Applications, 4th ed. Springer; 1998.
24. Williamson CHK, Govardhan R. Vortex-induced vibrations. Annual Review of Fluid Mechanics 2004; 36: 413–455. doi: 10.1146/annurev.fluid.36.050802.122128